Guided Ion Beam Studies of the Reactions of Ni^+, Cu^+, and Zn^+ with CS_2 and COS†

Chad Rue and P. B. Armentrout*

Department of Chemistry, University of Utah, Salt Lake City, Utah 84112

Ilona Kretzschmar,‡ Detlef Schröder, and Helmut Schwarz*

Institut für Chemie der Technischen Universität Berlin, Strasse des 17. Juni 135, D-10623 Berlin, Germany

Received: January 17, 2002; In Final Form: April 29, 2002

The reactions of atomic Ni^+, Cu^+, and Zn^+ with CS_2 and COS are studied using guided-ion beam mass spectrometry. Different ion sources are used to characterize the relative reactivities of different electronic states of Ni^+ and Cu^+. Ground-state ions of all three metals undergo endothermic reactions to form MS^+ from both CS_2 and COS, as well as MCS^+ and MCO^+, respectively. In several cases, the cross sections for forming MCX^+ (X = O, S) exhibit two endothermic features, which are assigned to the formation of different structural isomers or electronically excited product states. From the thresholds associated with forming MS^+ and MCS^+, we determine $D_0(Ni^+-S) = 2.46 \pm 0.04$, $D_0(Ni^+-CS) = 2.43 \pm 0.10$ eV, $D_0(Cu^+-S) = 2.07 \pm 0.15$, $D_0(Cu^+-CS) = 2.47 \pm 0.12$ eV, $D_0(Zn^+-S) = 2.05 \pm 0.12$, and $D_0(Zn^+-CS) = 1.54 \pm 0.24$ eV. The periodic trends in these values are discussed, and the nature of the bonding is analyzed. The results suggest that the initial mechanistic steps correspond to insertions of the metal ions into the C−S bonds of CXS (X = O, S).

Introduction

Nickel, copper, and zinc are among several transition metals that use sulfur coordination in some of their biological functions in various proteins and enzymes.[1,2] Despite the importance of metal−sulfur bonds, there is little fundamental information regarding transition-metal sulfides and their thermodynamic properties. One place to start such studies is the characterization of the simplest transition-metal sulfides, the diatomic MS^+ systems. In this work, we provide accurate measurements of the metal−sulfide bonds in the NiS^+, CuS^+, and ZnS^+ systems as part of an ongoing collaborative project to systematically examine the reactions of transition-metal cations with the sulfur-transfer reagents CS_2 and COS. Previous work[3] has established the thermochemistry of scandium,[4] titanium,[4] vanadium,[5,6] chromium,[7] manganese,[7] iron,[8−10] and cobalt[10] sulfide cations. The thermochemical results for these sulfides are included in Table 1 along with complementary literature thermochemistry needed in the present work. This study of the reactions of nickel, copper, and zinc cations with CS_2 and COS completes the 3d transition-metal ion series. M^+-S and M^+-CS bond energies for all three metals are derived and their bonding characteristics analyzed. Mechanisms for the reactions of the metal ions with CS_2 and COS are explored.

Experimental Section

Guided Ion Beam Mass Spectrometer. The experiments were performed with a guided-ion beam mass spectrometer (GIBMS), which has been described in detail previously.[11,12]

TABLE 1: Bond Dissociation Energies at 0 K

M	D_0(M−S), eV	D_0(M-CS), eV
C	7.37 (0.04)[a]	
CS	4.50 (0.04)[b]	
CO	3.140 (0.005)[b]	
Sc^+	4.97 (0.05)[c]	1.38 (0.08)[c]
Ti^+	4.74 (0.07)[c]	1.60 (0.06)[c]
V^+	3.72 (0.09)[d]	1.70 (0.08)[d]
Cr^+	2.68 (0.17)[e]	1.69 (0.06)[e]
Mn^+	2.52 (0.24)[e]	0.83 (0.22)[e]
Fe^+	3.08 (0.04)[f]	2.40 (0.12)[g]
Co^+	2.95 (0.09)[g]	2.68 (0.34)[g]
Ni^+	2.46 (0.04)[h]	2.43 (0.10)[h]
Cu^+	2.07 (0.15)[h]	2.47 (0.12)[h]
Zn^+	2.05 (0.12)[h]	1.54 (0.24)[h]

[a] Prinslow, D. A.; Armentrout, P. B. *J. Chem. Phys.* **1991**, *94*, 3563. [b] Pedley, J. B.; Naylor, R. D.; Kirby, S. P. *Thermochemical Data of Organic Compounds*; Chapman and Hall: London, 1986. Corrected to 0 K using $H° - H°$ (298.15) values taken from *JANAF Thermochemical Tables, Fourth Edition*; Chase, M. W., Ed.; *J. Phys. Chem. Ref. Data* **1998**, Monograph No. 9. [c] Kretzschmar et al., ref 4. [d] Kretzschmar et al., ref 6. [e] Rue et al., ref 7. [f] Schröder et al., ref 8. [g] Rue et al., ref 9. [h] This work.

Briefly, ions are produced in one of the sources described below, accelerated, and passed through a magnetic sector for mass selection. The mass-selected ion beam is then focused into the entrance of a radio frequency (rf) octopole ion guide, whose dc potential with respect to the ion source determines the kinetic energy of the ion beam. The rf potential on the octopole rods radially confines the ions and guides them through a gas cell, where a neutral reactant is introduced at pressures low enough (0.05−0.2 mTorr) to ensure single collision conditions. Both product and unreacted primary ions are extracted from the octopole and passed through a quadrupole for mass analysis. Finally, ions are detected with a secondary-electron scintillation ion detector and counted using standard pulse-counting techniques. This process is repeated at different collision energies

† Part of the special issue "Jack Beauchamp Festschrift". Dedicated to Professor J. L. Beauchamp on the ocassion of his 60th birthday and in thanks for his contributions throughout ion and physical chemistry.

* To whom correspondence should be addressed.

‡ Present address: Dept. Chem. & Chem. Biol., Harvard U., 12 Oxford St., Cambridge, MA 02138.

10.1021/jp020161k CCC: $22.00 © 2002 American Chemical Society
Published on Web 06/17/2002

simply by adjusting the dc octopole potential with respect to the ion source. Conversion of the raw ion intensities into cross sections and the calibration of the absolute energy scale are treated as described previously.[11] The accuracy of the product cross-section magnitudes is estimated to be ±20%, and the uncertainty in the absolute energy scale is ±0.05 eV (E_{lab}). Laboratory energies are converted to energies in the center-of-mass frame using $E_{CM} = E_{lab}\, M/(M + m)$, where M and m are the masses of the neutral and ionic reactants, respectively. This procedure accounts for conserving the momentum of the center-of-mass of the collision pair through the laboratory. Consequently, some of the laboratory ion energy is not available to the system to induce chemical changes.

Energy thresholds for product formation at zero Kelvin, E_0, are obtained by modeling the cross sections using eq 1

$$\sigma(E) = \sigma_0 \sum g_i (E + E_i - E_0)^n / E^m \qquad (1)$$

where σ_0 is an energy-independent scaling factor, E is the relative kinetic energy, and E_0 and n are treated as adjustable fitting parameters. The summation is over the rovibrational states of the neutral reactant having energies E_i and populations g_i ($\sum g_i = 1$). Before comparison to the experimental data, eq 1 is convoluted over the kinetic energy distributions of both reactants. Because the convoluted form of eq 1 explicitly accounts for all of the energy available to the reaction, the optimized value of E_0 is interpreted as the threshold energy at zero Kelvin. Uncertainties in the values of E_0 obtained using eq 1 are derived from the range of fitting parameters that yield acceptable fits coupled with the uncertainties in the absolute energy scale and electronic energies of the reactant ions.

Whereas the parameter m is typically held at unity,[13] previous investigations of the $V^+ + CS_2$ reaction have demonstrated that a value of $m = 1.5$ is more appropriate for the description of spin-forbidden processes.[5] Several of the reactions discussed in the present work are spin-forbidden (see below), and each of these is modeled using eq 1 with $m = 1.5$ in addition to $m = 1$.

Ion Sources. Briefly, M^+ (M = Ni, Cu, and Zn) ions are formed in either a dc discharge/flow tube (DC/FT) source or a surface ionization (SI) source. In the DC/FT source, energetic Ar^+ ions sputter M^+ ions from a negatively charged (−1.5 to −2 kV) cathode composed of the metal to be studied. The ions formed in this discharge are then swept through a meter-long flow tube by a 10% argon in helium buffer gas at a total pressure of 0.7−1 Torr. The ions undergo ~10^5 collisions with the buffer gas as they traverse the flow tube, which helps to cool the ions to room temperature. Previous studies indicate that excited states of Zn^+ (Table 2) comprise less than 0.01% of the ions produced in this source.[14] For the other metal ions, it has been shown that helium and argon are not always effective at quenching the excited electronic states of transition-metal ions.[3−10,15] Therefore, small amounts (40 mTorr or less) of a cooling gas (O_2 for Ni^+ and NO for Cu^+) are added to the flow tube to react with and thus remove excited states from the M^+ beam. Previous studies have demonstrated that oxygen quenches the electronic states of Ni^+ such that the average electronic energy is less than 0.02 eV.[16] For Cu^+, the addition of NO is found to eliminate excited states almost completely,[14,17] and the results discussed below indicate that cooling with NO reduces the excited-state population to less than 0.3% of the beam intensity. Because of the negligible amount of excited states, no explicit contribution of such electronic excitation is included in the analyses below, but the final threshold values cited for Ni^+ include the average electronic excitation energy as part of their uncertainties. For convenience in the following, we will refer to ions produced in the DC/FT source with and without the appropriate additional cooling gases (O_2 or NO) as cooled and uncooled.

TABLE 2: Electronic States of First Row Transition-Metal Ions

ion	state	configuration	energy (eV)[a]	2425 K[b]
Ni^+	^2D	$3d^9$	0.075	98.3806
	^4F	$3d^8\ 4s^1$	1.160	1.5754
	^2F	$3d^8\ 4s^1$	1.757	0.0438
	^4P	$3d^8\ 4s^1$	2.970	0.0001
Cu^+	^1S	$3d^{10}$	0.000	
	^3D	$3d^9\ 4s^1$	2.808	
	^1D	$3d^9\ 4s^1$	3.256	
	$^3P°$	$3d^9\ 4p^1$	8.330	
Zn^+	^2S	$3d^{10}\ 4s^1$	0.000	
	$^2P°$	$3d^{10}\ 4p^1$	6.083	
	^2D	$3d^9\ 4s^2$	7.911	
	^2S	$3d^{10}\ 5s^1$	10.965	

[a] Energies are weighted averages (by degeneracies) over spin−orbit levels. Values calculated from spin−orbit level energies given in http://physics.nist.gov/cgi-bin/AtData/main_asd. [b] Population of electronic states of Ni^+ in percent at the specified temperature.

In the present study, the SI source was also used to form Ni^+. This source involves vaporizing $NiCl_2$ in an oven and directing the vapor at a resistively heated rhenium filament. The compound decomposes on the filament, and Ni^+ ions desorb. The electronic states of Ni^+ thus formed are assumed to have a Boltzmann distribution characteristic of the filament temperature. The filament temperature was previously calibrated as a function of the applied current using optical pyrometry, assuming that the filament acts as a blackbody radiator.[18] Because the low-lying electronic states of Ni^+ involve only s and d orbitals, spontaneous optical emission from excited states are parity forbidden, such that the excited-state lifetimes are expected to be longer than the ~1 ms residence time of the ions in the instrument.[19] Therefore, the Ni^+ state distribution is determined by the SI filament temperature, which can be systematically adjusted from 2150 to 2400 K. Below 2150 K, the Ni^+ beam intensity is unacceptably low (<10^3 counts s^{-1}), and above 2400 K, the filament burns out rapidly. This narrow temperature range, combined with the relatively low beam intensities produced by $NiCl_2$, results in poor signal-to-noise levels and large uncertainties in the cross sections. Nevertheless, we performed the $Ni^+ + CS_2$ reaction with Ni^+ ions generated at SI filament temperatures of 2150, 2200, 2250, 2350, and 2425 K. Because the results obtained were much noisier than the DC/FT data and by and large comparable at various temperatures examined, only the 2425 K data are discussed explicitly. The populations of states produced at 2425 K are listed in Table 2.

Results

Reactions of M^+ with CS_2. The product cross sections observed in the reactions of CS_2 with M^+ formed using the DC/FT source with cooling gases added are shown in Figures 1−3 for Ni^+, Cu^+, and Zn^+, respectively. For Cu^+, the threshold data have been corrected for residual contributions from excited states (see discussion below). Three primary product ions are formed in all three systems in the endothermic reactions 2−4:

$$M^+ + CS_2 \rightarrow MS^+ + CS \qquad (2)$$

$$\rightarrow [M,C,S]^+ + S \qquad (3)$$

$$\rightarrow CS_2{}^+ + M \qquad (4)$$

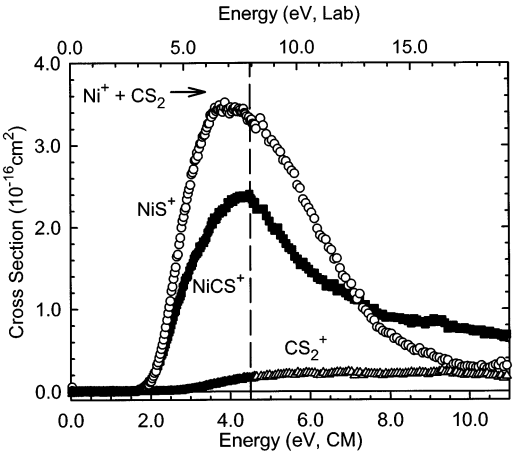

Figure 1. Product cross sections for the formation of NiS^+ (open circles), $NiCS^+$ (closed squares), and CS_2^+ (open triangles) in the reaction of $Ni^+ + CS_2$ as a function of kinetic energy in the center-of-mass (lower *x* axis) and laboratory (upper *x* axis) frames. Nickel ions are formed in the DC/FT source with O_2 cooling gas present. The bond dissociation energy of CS_2 (4.50 eV) is marked by the broken line.

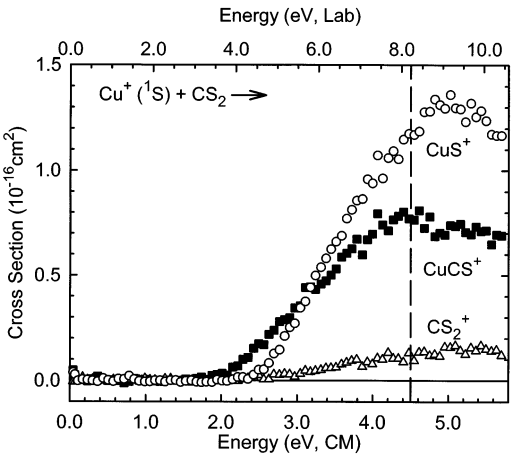

Figure 2. Product cross sections for the formation of CuS^+ (open circles), $CuCS^+$ (closed squares), and CS_2^+ (open triangles) in the reaction of $Cu^+ + CS_2$ as a function of kinetic energy in the center-of-mass (lower *x* axis) and laboratory (upper *x* axis) frames. Copper ions are formed in the DC/FT source with NO cooling gas present, and residual contributions from excited states have been subtracted out as described in the text. The bond dissociation energy of CS_2 (4.50 eV) is marked by the broken line.

The brackets indicate that the structure of the $[M,C,S]^+$ species is not yet defined, however, it can safely be assigned as the metal-thiocarbonyl cation, M^+-CS, at the lowest energies[5,20]

Charge transfer to form CS_2^+, reaction 4, is observed in all three systems. The ionization energy (IE) of CS_2 is 10.073 ± 0.005 eV, compared with IE(Ni) = 7.6398, IE(Cu) = 7.72638 $\pm$ 0.00001 eV, and IE(Zn) = 9.39405 eV.[21] Thus, reaction 4 is endothermic in all three cases with expected thresholds of 2.43, 2.35, and 0.68 eV for reactions with Ni^+, Cu^+, and Zn^+, respectively. This corresponds reasonably well with the apparent thresholds in all three systems, confirming that these data contain little contributions from excited electronic states of the metal ions. Indeed, analysis of these data channels using eq 1 provides thresholds of 2.57 ± 0.21, 2.26 ± 0.56, and 0.92 ± 0.17 eV (Table 3), in reasonable agreement with the predicted thresholds. In the Zn^+/CS_2 system, the threshold for charge exchange is sufficiently low that this process dominates the product spectrum. The CS_2^+ cross section is observed to decline above 6 eV, for reasons that are unclear. It is possible that this is an artifact associated with incomplete collection of CS_2^+, which probably has a small velocity in the laboratory frame.

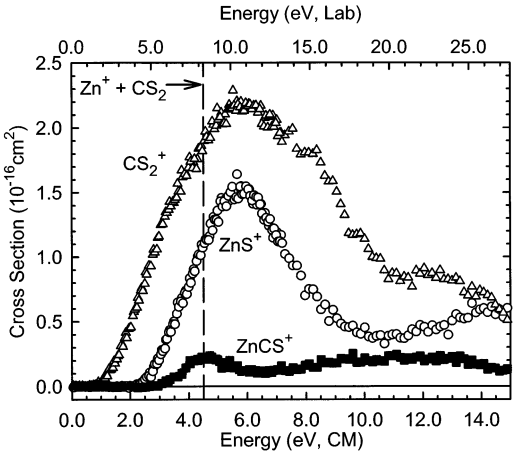

Figure 3. Product cross sections for the formation of ZnS^+ (open circles), $ZnCS^+$ (closed squares), and CS_2^+ (open triangles) in the reaction of $Zn^+ + CS_2$ as a function of kinetic energy in the center-of-mass (lower *x* axis) and laboratory (upper *x* axis) frames. Zinc ions are formed in the DC/FT source. The bond dissociation energy of CS_2 (4.50 eV) is marked by the broken line.

TABLE 3: Optimized Parameters of eq 1

reaction	products	σ_0	E_0	n	m
$Ni^+ + CS_2$	NiS^+	8.1 (1.3)	2.21 (0.07)	1.1 (0.2)	1
		13 (2)	2.19 (0.08)	1.2 (0.2)	1.5
	$NiCS^+$	3.8 (0.6)	2.07 (0.09)	1.2 (0.2)	1
	CS_2^+	0.28 (0.10)	2.57 (0.21)	1.7 (0.5)	1
$Ni^+ + COS$	NiS^+	5.2 (0.1)	0.70 (0.03)	0.55 (0.07)	1
		6.5 (0.1)	0.66 (0.03)	0.85 (0.06)	1.5
	$NiCO^+$	1.2 (0.3)	1.77 (0.16)	1.3 (0.4)	1
$Cu^+ + CS_2$	CuS^+	2.8 (0.4)	2.70 (0.09)	1.1 (0.2)	1
		5.3 (0.5)	2.69 (0.06)	1.3 (0.1)	1.5
	$CuCS^+$	1.0 (0.2)	2.03 (0.11)	1.5 (0.2)	1
	CS_2^+	0.18 (0.13)	2.26 (0.56)	1.6 (0.7)	1
$Cu^+ + COS$	CuS^+	0.42 (0.12)	1.08 (0.14)	2.3 (0.3)	1
		0.56 (0.22)	1.05 (0.16)	2.7 (0.4)	1.5
	$CuCO^+$	0.11 (0.03)	1.57 (0.32)	1.4 (0.6)	1
$Zn^+ + CS_2$	ZnS^+	1.6 (0.4)	2.45 (0.14)	1.8 (0.3)	1
	$ZnCS^+$	0.52 (0.20)	2.96 (0.23)	1.8 (0.7)	1
	CS_2^+	0.83 (0.31)	0.92 (0.17)	2.0 (0.3)	1
$Zn^+ + COS$	ZnS^+	0.69 (0.22)	1.09 (0.12)	2.2 (0.3)	1

In the following, we shall concentrate on the differences in the apparent thresholds for MS^+ and $[M,C,S]^+$ formations (Figures 1−3). Analyses of the cross sections in the Ni^+/CS_2 system using eq 1 (Table 3) leads to threshold values of 2.20 $\pm$ 0.08 eV (average of $m = 1$ and 1.5 fits) for reaction 2 and 2.07 ± 0.09 eV for reaction 3. In marked contrast, the threshold of 2.03 ± 0.11 eV for $CuCS^+$ formation is lower than the threshold of 2.69 ± 0.08 eV (average of $m = 1$ and 1.5 fits) for CuS^+ formation. In the Zn^+/CS_2 system, the ordering is reversed, and thresholds of 2.45 ± 0.14 and 2.96 ± 0.23 eV are derived from the cross sections for ZnS^+ and $ZnCS^+$, respectively.

At kinetic energies above the threshold for product formation, the excess energy can enter the internal modes of the ionic products. Eventually, enough excess internal energy is deposited to induce dissociation according to the overall reaction 5:

$$M^+ + CS_2 \rightarrow M^+ + S + CS \qquad (5)$$

The thermodynamic onset for reaction 5 is equivalent to the

bond energy of CS_2, 4.50 ± 0.04 eV (Table 1). In all three M^+/CS_2 systems, the MCS^+ cross sections begin to decline close to this energy, partly because the atomic S neutral product has no internal degrees of freedom (other than electronic) with which to carry away energy. This is also true for the NiS^+ cross section, whereas the cross sections for formation of CuS^+ and ZnS^+ decline at slightly higher energies. One explanation for these latter observations is that the neutral CS product fragments formed in reactions 2 carry away a fraction of the available energy when M = Cu or Zn.

Another interesting explanation is related to previous observations regarding so-called "impulsive" behavior in the reactions of Cu^+ and Zn^+ with several small molecules.[13,17,22] This phenomenon is related to the duration of the collision interaction. Thus, in most collisions, the energy available to the intermediate MCS_2^+ collision complexes randomizes efficiently, leading to dissociation process 5 beginning at the thermodynamic limit. However, if the collision complex is very short-lived, the metal may interact primarily with the first atom it encounters on the neutral target. In the extreme limit of an "impulsive" interaction, the remaining atoms of the neutral are isolated from the collision event. The energy conversion from the laboratory frame for a purely impulsive collision is such that less energy is available for reaction because some energy is retained in translation. This shifts the cross section features to higher energies. The present results suggest that mildly impulsive reactivity is involved in the Cu^+ and Zn^+ systems, much like that previously observed for reaction of the isovalent $Cu^+ + CO_2$ system,[17] such that the lifetimes of the collision complexes for these metals are short relative to those of Ni^+. This may be associated with the Pauli repulsion between the closed-shell CS_2 molecule and the occupied 4s orbital on Zn^+, which has a $3d^{10}4s^1$ electron configuration. Impulsive reactivity may arise in the Cu^+/CS_2 system, because the closed shell $Cu^+(^1S, 3d^{10})$ species is relatively stable and does not easily insert into the bonds of the neutral target.[23]

In the reaction of Zn^+ with CS_2 (Figure 3), the $[Zn,C,S]^+$ cross section exhibits a distinct second feature with a threshold near 6−7 eV. Similar behavior has been observed for the reactions of V^+,[5] Cr^+,[7] Mn^+,[7] Fe^+,[10] and Co^+ [10] with CS_2, where it has been attributed to the formation of the $C-M^+-S$ isomer. This assignment is consistent with the observation that the second feature of the $[Zn,C,S]^+$ cross section declines near the onset of a second endothermic feature of the ZnS^+ channel. This correlation could indicate that $C-Zn^+-S$ is the precursor for ZnS^+ at higher energies, consistent with cleavage of the $C-ZnS^+$ bond to form ZnS^+ according to reaction 6:

$$Zn^+ + CS_2 \rightarrow ZnS^+ + C + S \qquad (6)$$

The position of the second feature in the ZnS^+ cross section is in reasonable agreement with the thermodynamic threshold of 9.82 ± 0.15 eV for reaction 6 (Table 1). However, the electronic structure of Zn^+ (^2S, $3d^{10}4s^1$) disfavors formation of covalent bonds to both C and S. One possible alternative structure is a cyclic $[Zn,C,S]^+$ isomer.

In addition, we also consider whether this high-energy feature could be assigned to formation of an excited electronic state of $ZnCS^+$. This possibility can be explored by a qualitative consideration of the possible excited states of the $[Zn,C,S]^+$ product. To understand this, we note that coupling of $Zn^+(^2S, 3d^{10}4s^1)$ with $CS(^1\Sigma^+)$ can form only a single electronic state of $ZnCS^+$, likely to be $^2\Sigma^+$. Thus, putative excited states of $ZnCS^+$ must evolve from excited states of Zn^+ (Table 2) or

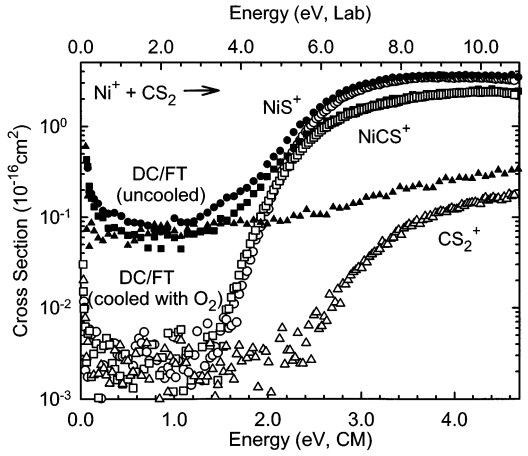

Figure 4. Product cross sections for the formation of NiS^+ (circles), $NiCS^+$ (squares), and CS_2^+ (triangles) in the reaction of $Ni^+ + CS_2$ as a function of kinetic energy in the center-of-mass (lower *x* axis) and laboratory (upper *x* axis) frames. Results are shown for nickel ions formed in the DC/FT source with O_2 cooling gas present (open symbols) and without (closed symbols).

CS. Coupling of $Zn^+(^2P^o, 3d^{10}4p^1)$ with $CS(^1\Sigma^+)$ should lead to $^2\Sigma^+$ and $^2\Pi$ states, where the former should have a weak bond and the latter will be strongly bound with a bond energy comparable to $Cu^+(^1S, 3d^{10})$. This provides sufficient information to estimate the electronic excitation energy of $ZnCS^+$, ΔE_{ZnCS^+}, according to eq 7:

$$\Delta E_{ZnCS^+} = \Delta E_{Zn^+} + D_{0,g}(Zn^+-CS) - D_{0,e}(Zn^+-CS) \qquad (7)$$

where ΔE_{Zn^+} is the $Zn^+(^2P^o) \leftarrow Zn^+(^2S)$ excitation energy of 6.08 eV (Table 2)[24] and $D_{0,g}(Zn^+-CS)$ and $D_{0,e}(Zn^+-CS) \approx D_0(Cu^+-CS)$ are the bond energies of the ground and excited states of $ZnCS^+$, respectively. Given the bond energies in Table 1, this suggests that ΔE_{ZnCS^+} is approximately 5.2 ± 0.3 eV, which means that the threshold for formation of $ZnCS^+(^2\Pi)$ is 8.1 ± 0.4 eV, well above the observed threshold for the higher energy feature in the $[Zn,C,S]^+$ cross section. Alternatively, we can view the $^2\Pi$ state of $ZnCS^+$ as coming from a covalent coupling of $Zn^+(^2S, 3d^{10}4s^1)$ with $CS(^1\Pi)$, 4.8 eV above ground-state $CS(^1\Sigma^+)$.[25] If this two-electron bond is again estimated as equivalent to that for the two-electron bond in Cu^+-CS, then ΔE_{ZnCS^+} is ≈ 3.9 ± 0.3 eV, consistent with the energy differences in the cross section features. Therefore, the assignment of the higher energy feature in the $[Zn,C,S]^+$ cross section to a $^2\Pi$ excited state is plausible.

Electronic Distributions of the Ni^+ Reactants. The reactions of CS_2 with Ni^+ ions formed under different source conditions are shown in Figure 4. When no O_2 cooling gas is added to the flow tube, all three product cross sections exhibit low-energy features that increase slightly in magnitude with decreasing energy, characteristic of exothermic processes. These low-energy cross sections are about a factor of 60 larger than those observed when O_2 cooling gas is present. We also examined these reactions with Ni^+ formed using the SI source. Table 2 gives the Boltzmann populations of the various Ni^+ states at 2425 K. In all cases, the SI data are noisier because the intensity of the ion beams is smaller than with the DC/FT source. At low energies, the SI data fall between the data taken with cooled and uncooled DC/FT conditions. We observed no distinct excited-state features in the cross sections, although the thresholds for reaction of Ni^+(SI) are clearly lower than those for reaction of Ni^+ ions formed in the O_2-cooled DC/FT source.

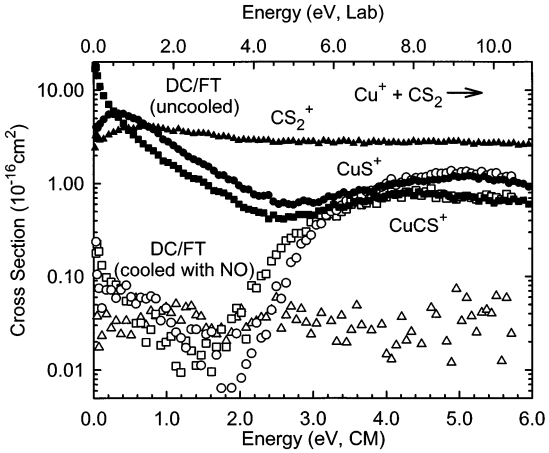

Figure 5. Product cross sections for the formation of CuS^+ (circles), $CuCS^+$ (squares), and CS_2^+ (triangles) in the reaction of $Cu^+ + CS_2$ as a function of kinetic energy in the center-of-mass (lower *x* axis) and laboratory (upper *x* axis) frames. Results are shown for copper ions formed in the DC/FT source with NO cooling gas present (open symbols) and without (closed symbols).

These observations are consistent with the presence of small amounts of excited Ni^+ in the ion beam (Table 2). For all SI and DC/FT source conditions, the primary endothermic features observed at energies above 2 eV are present with comparable magnitudes for all three product ions. This behavior unambiguously establishes that these features result from reaction of the $Ni^+(^2D)$ ground state.

As noted above, the thresholds for product formation in the $Ni^+(^2D) + CS_2$ system exceed 2 eV for all three products. These threshold energies are higher than the excitation energy from the ^2D ground state to the ^4F and ^2F excited states of Ni^+ (1.09 and 1.68 eV, respectively, Table 2), indicating that these excited states should also react endothermically. Therefore, the exothermic feature observed using the uncooled DC/FT source must result from reaction of the $Ni^+(^4P)$ (2.97 eV above the ground state) and/or higher-lying states. The combined magnitude of the exothermic features in the product cross sections obtained using the uncooled DC/FT source is $0.3 \pm 0.1\%$ ($0.005 \pm 0.003\%$ for the cooled data) of the Langevin−Gioumousis−Stevenson (LGS) cross section,[26] which is an estimate of the ion−molecule collision probability. Because the observed cross sections only arise from reactive collisions, this percentage is regarded as a lower limit to the population of the ^4P and higher states in the beam of Ni^+ ions generated by the uncooled DC/FT. Clearly, these states are not efficiently thermalized by collisions with the helium/argon bath gas in the flow tube, but can effectively be removed upon addition of O_2.

Electronic Distributions of the Cu^+ Reactants. The CuS^+, $[Cu,C,S]^+$, and CS_2^+ cross sections observed in the $Cu^+ + CS_2$ reaction are shown in Figure 5. When Cu^+ ions are formed using the DC/FT source without adding a cooling gas to the flow tube, all three cross sections exhibit large features at low energies. When NO is added to the flow tube as a cooling gas,[14,17] these low-energy features uniformly decrease by about 2 orders of magnitude and are assigned to excited-state Cu^+. Previous work in our laboratory confirms that the $Cu^+(^3D)$ first excited state is formed by the dc discharge.[17] In addition, the ionization energy of CS_2 is 10.073 ± 0.005 eV, 2.347 eV above that of Cu, 7.72638 ± 0.00001 eV.[21] However, ionization to form the ^3D state of Cu^+ requires 2.81 eV more energy,[24,27] such that the charge-transfer reaction with CS_2 is nearly resonant with this state (which has spin−orbit levels that span about 0.26 eV). The slight mismatch in ionization energies may partially explain why the CS_2^+ cross section increases slightly with increasing kinetic energy, despite being exothermic.

Without a cooling gas, the reaction of Cu^+ to form $[Cu,C,S]^+$ appears to be exothermic and barrierless, whereas the CuS^+ and CS_2^+ cross sections decrease as the energy is reduced below 0.2 and 0.4 eV, respectively, suggesting that these reactions are slightly endothermic and/or kinetically hindered. Analyses of the cooled and uncooled data using eq 1 yields thresholds for the ground and excited-state features in the CuS^+ cross section of 2.69 ± 0.08 and 0.14 ± 0.05 eV, respectively. The energy difference of 2.55 ± 0.09 eV for these features is reasonably consistent with the known energy difference of 2.72 eV between the $Cu^+(^1S)$ ground state and the lowest spin−orbit level ($J = 3$) of the $Cu^+(^3D)$ first excited state,[27] although the average energy difference between these states (including all spin−orbit levels) is slightly higher (2.81 eV, Table 2). The observation that the threshold energy difference between the ground and excited-state features in the CuS^+ cross section does not precisely match the $Cu^+(^1S) \leftarrow Cu^+(^3D)$ excitation energy is attributed to competition with reaction 3. Competition may also explain the observation of apparent endothermic behavior in the exothermic charge-transfer reaction between $Cu^+(^3D)$ and CS_2. Reaction 3 is exothermic for the $Cu^+(^3D)$ excited state by about 0.7 eV, which would make it much more efficient than process 2, thereby shifting the threshold for $Cu^+(^3D)$ to slightly higher energies.

The total cross section for reaction of $Cu^+(^3D)$ (not shown) declines smoothly with increasing energy as $E^{-0.5}$ from about 0.7 to 2.5 eV, as predicted by the LGS model,[26] but with an absolute magnitude of 30% of the predicted cross section. This percentage represents a lower limit to the fraction of excited states present in the ion beam; however, the cross sections above 3 eV (attributable to reaction of the ^1S ground state) are comparable in magnitude whether the cooling gas is present. This observation indicates that there must still be a large fraction of ground-state Cu^+ in the uncooled ion beam, such that the 30% lower limit cannot be appreciably higher than this. At energies below 0.7 eV, the total cross section declines less rapidly than $E^{-0.5}$, a consequence of the apparent endothermicity of the reaction forming CuS^+ and the inefficiency of the charge-transfer reaction. At higher energies, the total cross section levels out at a magnitude of about 3 Å^2, largely to form the charge-transfer product. We note that small exothermic tails remain in many of our data sets for Cu^+ even with the addition of NO to the flow tube. Nevertheless, the contribution of these residual excited states is not problematic, because their energy dependences are distinct from that of the ground state. In cases where cooling with NO is incomplete, the excited-state features are modeled separately and subtracted from the data. This provides a good estimate of the ground-state Cu^+ cross sections, as shown in Figure 2.

Electronic Distributions of the Zn^+ Reactants. Unlike the Ni^+ and Cu^+ systems, the addition of cooling gases to the flow tube did not affect the product cross sections in the reactions of Zn^+ with CS_2 or COS. It is possible that the collisions with helium and argon in the flow tube are efficient at quenching the excited states of Zn^+, that these states are not formed in the discharge, or that the excited states decay rapidly. Formation of excited states is probably inhibited by the large excitation energies involved, e.g., the $^2P°$ first excited state of Zn^+ lies 6.08 eV above the ground state, Table 2. In addition, this $^2P°(3d^{10}4p^1)$ state has a dipole-allowed transition to the $^2S(3d^{10}4s^1)$ ground-state such that its radiative lifetime should be very short.

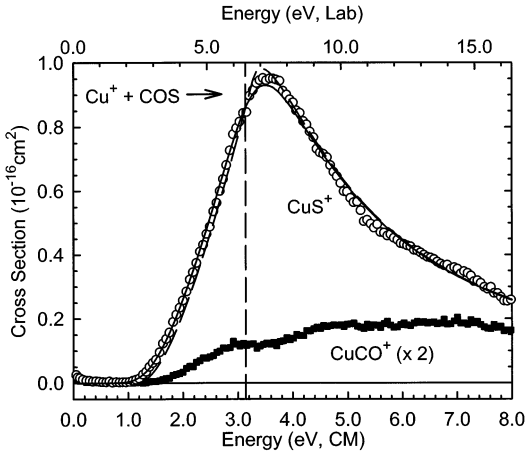

Figure 6. Product cross sections for the formation of CuS^+ (open circles) and $CuCO^+$ (closed squares, multiplied by a factor of 2) in the reaction of $Cu^+ + COS$ as a function of kinetic energy in the center-of-mass (lower *x* axis) and laboratory (upper *x* axis) frames. Copper ions are formed in the DC/FT source with NO cooling gas present. The bond dissociation energy of S−CO (3.14 eV) is marked by the vertical broken line. The full line indicates the model of eq 1 using the parameters given in Table 3 ($m = 1.5$) convoluted over the kinetic energy distributions of the reactants. The dashed line shows this model for reactants with no internal or kinetic energy distributions. Above 3.14 eV, a model for the subsequent dissociation process is also included.

Other excited states of Zn^+ can also radiate in dipole-allowed transitions to either the ground or first excited-state such that no excited states of Zn^+ are expected to live long enough to reach the reaction cell, whereas radiative transitions are parity forbidden for the excited states of Ni^+ and Cu^+ considered above. Consequently, the cross sections observed for reaction of Zn^+ certainly correspond to the reaction of the ^2S ground state.

Reactions of Cu^+ with COS. In terms of the reactions observed, the reactivity of COS toward Cu^+ generated in the DC/FT source with NO cooling gas is generally similar to the behavior observed in the M^+/CS_2 system, except that charge transfer to yield COS^+ is absent. The formations of CuS^+ and $[Cu,C,O]^+$ in reactions 8 and 9, analogous to reactions 2 and 3, respectively, are observed (Figure 6):

$$Cu^+ + COS \rightarrow CuS^+ + CO \quad (8)$$

$$\rightarrow [Cu,C,O]^+ + S \quad (9)$$

Product ions such as COS^+, CuO^+, and $CuCS^+$ were looked for and not observed.

Note the difference between the relative thresholds of the MCX^+ (X = S, O) and MS^+ products in the Cu^+/CS_2 and Cu^+/COS systems. $CuCS^+$ formation precedes CuS^+ formation in the CS_2 reaction, but CuS^+ precedes $CuCO^+$ in the reaction with COS (Figures 2 and 6). This behavior is a direct reflection of the relative bond energies (see below). Analyses of these cross sections using eq 1 gives the optimized parameters summarized in Table 3. Near 3.14 eV, the CuS^+ cross section begins to decline, and the $CuCO^+$ cross section levels out, in good agreement with the thermodynamic onset for COS dissociation (Table 1) according to reaction 10:

$$Cu^+ + COS \rightarrow Cu^+ + S + CO \quad (10)$$

The reproduction of the data shown in Figure 6 for the CuS^+ channel modifies eq 1 above 3.14 eV to include a simple statistical treatment of this subsequent dissociation, as detailed elsewhere.[28]

The $[Cu,C,O]^+$ channel exhibits two features. The lower threshold certainly corresponds to formation of ground-state Cu^+-CO. Indeed, the threshold measured for this process, 1.57 ± 0.32 eV (Table 3), is in good agreement with a 1.60 ± 0.07 eV value calculated from a previously reported value of $D_0(Cu^+-CO) = 1.54 \pm 0.07$ eV.[29] Accordingly, we conclude that formation of $CuCO^+$ in the Cu^+/COS system is not significantly hindered by competition with the thermochemically favored CuS^+ channel.

The higher energy feature in the $[Cu,C,O]^+$ cross section could conceivably be assigned to an excited electronic state of $CuCO^+$, but such an assignment seems inconsistent with the energy difference of approximately 2 eV between the observed cross section features. To understand this, we first note that coupling of ground-state $Cu^+(^1S)$ and $CO(^1\Sigma^+)$ can form only a single electronic state of $CuCO^+$, calculated to be $^1\Sigma^+$.[30] Hence, excited states of $CuCO^+$ must evolve from excited states of CO or Cu^+. The first known excited state of CO lies over 8 eV above the ground state,[25] such that plausible excited states of $CuCO^+$ probably originate from the $^3D(3d^9 4s^1)$ first excited state of Cu^+, which lies 2.81 eV above the ground state (Table 2). Because of the occupation of the 4s orbital in this state, interaction of CO with $Cu^+(^3D)$ is probably less attractive than with $Cu^+(^1S)$, such that the bond energies of triplet excited states of $CuCO^+$ should be less than those of the singlet ground state. Therefore, the excitation energy of $CuCO^+$ probably exceeds the asymptotic value for Cu^+ of 2.81 eV, which appears inconsistent with the energy difference observed for the features in the $CuCO^+$ cross section. We might also attribute the high energy feature in the $[Cu,C,O]^+$ cross section to the formation of a $C-Cu^+-O$ isomer, but formation of such covalent bonds also requires promotion of the closed shell $Cu^+(^1S, 3d^{10})$, and in addition, the very strong CO bond must be broken. At this point, the assignment of the high-energy feature in this cross section remains uncertain.

Reactions of Zn^+ with COS. The cross section for ZnS^+ formation in the reaction with COS is shown in Figure 7. Other product ions such as COS^+, ZnO^+, $ZnCS^+$, and $ZnCO^+$ were looked for and not observed. The main differences between the reactions of Zn^+ with CS_2 and COS are that neither CXS^+ nor $ZnCX^+$ formation are observed in the latter system. These observations certainly indicate that $ZnCO^+$ formation is disfavored, a result that can also be appreciated from the relative magnitudes of the cross sections for the analogous reactions in the Cu^+ system. It is unlikely that the initial insertion into the S−CO bond is problematic, because $ZnCS^+$ is formed in the reaction of Zn^+ with CS_2, which has a higher C−S bond energy (4.50 vs 3.14 eV, Table 1). Instead, this behavior is assigned to be a consequence of the relative thermodynamics, namely, the $ZnCO^+$ species is weakly bound, consistent with the discussion below for the isovalent $ZnCS^+$ species. In this regard, the failure to observe $ZnCO^+$ in the reaction of $Zn^+(3d^{10}4s^1)$ with COS is analogous to our failure to observe $MnCO^+$ in the reaction of $Mn^+(3d^5 4s^1)$ with COS.[7] In both cases, this is because the occupied 4s orbital means that neither Zn^+ nor Mn^+ has an empty orbital to accept electron density from the CO ligand. Thus, selective cleavage of the $S-M^+-CO$ insertion intermediate bond to form MCO^+ is disfavored.

Reactions of Ni^+ with COS. The product cross sections observed in the reaction of COS with Ni^+ generated in the DC/FT source are shown in Figure 8. Other product ions such as

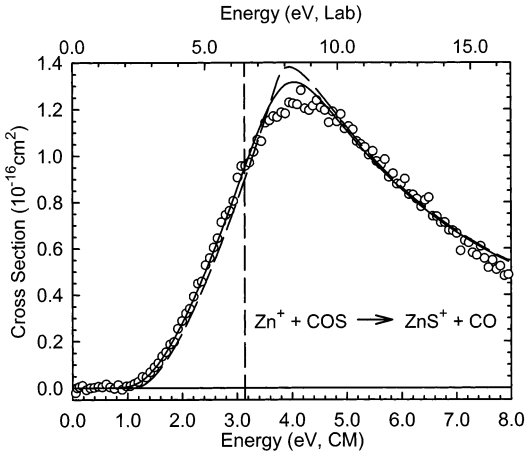

Figure 7. Product cross sections for the formation of ZnS^+ (open circles) in the reaction of $Zn^+ + COS$ as a function of kinetic energy in the center-of-mass (lower *x* axis) and laboratory (upper *x* axis) frames. Zinc ions are formed in the DC/FT source. The bond dissociation energy of S−CO (3.14 eV) is marked by the vertical broken line. The full line indicates the model of eq 1 using the parameters given in Table 3 ($m = 1.5$) convoluted over the kinetic energy distributions of the reactants. The dashed line shows this model for reactants with no internal or kinetic energy distributions. Above 3.14 eV, a model for the subsequent dissociation process is also included.

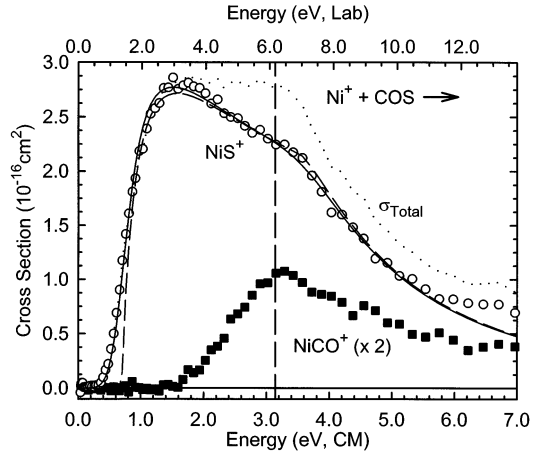

Figure 8. Product cross sections for the formation of NiS^+ (open circles), $NiCO^+$ (closed squares, multiplied by a factor of 2), and the total cross section (dotted line) in the reaction of $Ni^+ + COS$ as a function of kinetic energy in the center-of-mass (lower *x* axis) and laboratory (upper *x* axis) frames. Nickel ions are formed in the DC/FT source with O_2 cooling gas present, and residual contributions from excited states have been subtracted out as described in the text. The bond dissociation energy of S−CO (3.14 eV) is marked by the vertical broken line. The full line indicates the model of eq 1 using the parameters given in Table 3 ($m = 1.5$) convoluted over the kinetic energy distributions of the reactants. The dashed line shows this model for reactants with no internal or kinetic energy distributions. Above 3.14 eV, a model for the subsequent dissociation process is also included.

COS^+, NiO^+, and $NiCS^+$ were looked for and not observed. Small contributions from excited states leading to exothermic reactivity have been subtracted out by fitting these with a power law. The cross section for NiS^+ formation has an unusual energy dependence and rises very rapidly compared to the analogous cross sections for CuS^+ and ZnS^+ formation. This is evident by inspection of Figures 6−8 and in the optimized values of the fitting parameter *n* in eq 1 (Table 3). Higher values of *n* correspond to more slowly rising cross sections, and typical values of *n* range from 1 to 2. The optimized values of *n* for the CuS^+ and ZnS^+ cross sections in the reactions with COS are 2.3 ± 0.3 and 2.2 ± 0.3 ($m = 1$ fits), respectively. The value of *n* for the NiS^+ cross section, however, is considerably lower at 0.55 ± 0.07 ($m = 1$).

The NiS^+ cross section begins to decline around 1.5 eV, partially because of the competitive formation of $NiCO^+$. However, the total cross section also levels out near 1.5 eV, which indicates a significant change in the total reactivity of the system. The rapid decline in the cross sections at higher energies (above ∼3.0 eV) is attributed to simple dissociation in reaction 11:

$$Ni^+ + COS \rightarrow Ni^+ + S + CO \qquad (11)$$

Although the decline above 3.14 eV is expected, the strong decrease of the NiS^+ cross section and the abrupt slope change in the total cross section near 1.5 eV cannot be explained by dissociative or competitive processes. Instead, we must consider the details of the potential-energy surface.

Theoretical calculations indicate that the NiS^+ molecule has a $^4\Sigma^-$ ground state.[3] Thus, the formation of ground-state products from ground-state reactants in reaction 12 is formally spin-forbidden:

$$Ni^+(^2D) + COS(^1\Sigma) \rightarrow NiS^+(^4\Sigma^-) + CO(^1\Sigma) \qquad (12)$$

Provided there is sufficient coupling between the doublet diabatic potential-energy surface in the reactant region and the quartet potential-energy surface in the product region, the reaction can proceed along the adiabatic pathway and undergo spin-inversion with relative efficiency. This is especially true when the total energy of the system is close to the energy of the crossing point, because the residence time at the intersection will be long enough to allow for the necessary electronic reorganizations between spin surfaces. At higher kinetic energies, the probability of spin-inversion decreases, and it becomes increasingly likely that the reaction will retain its original spin, remain on the doublet potential-energy surface, and return to reactants via the entrance channel. We propose that the decreased probability for spin inversion at higher kinetic energies is responsible for the decreasing NiS^+ and total cross sections observed in the Ni^+/COS system between 1.5 and 3 eV.[5,31]

Previous studies of the $V^+ + CS_2$ system showed similar behavior,[5] and demonstrated that the cross section for forming the spin-forbidden VS^+ product can be adequately reproduced by eq 1 when a value of $m = 1.5$ is used. The use of $m = 1.5$ in eq 1 (instead of the usual $m = 1$) is mathematically equivalent to multiplying our normal fitting equation by $E^{-1/2}$, which is intended to account for the energy dependence of the probability for spin-inversion at energies above the surface crossing point.[5,32,33] Thus, the use of $m = 1.5$ in eq 1 provides a better fit to the data of sharply rising spin-forbidden cross sections (such as the NiS^+ cross section in the COS system and the VS^+ cross section observed in the reaction of V^+ with CS_2).[5] Figure 8 illustrates that the NiS^+ cross section can be reproduced well over an extended energy range using eq 1 when $m = 1.5$. (Above 3.14 eV, the reproduction of the data shown modifies eq 1 by including a simple statistical model described elsewhere[28] to account for the effects of the dissociation channel, reaction 11.) In contrast, modeling with $m = 1$ fails to reproduce the data above 1.5 eV.

However, reaction 12 is not the only spin-forbidden process considered in this work. Likewise, reactions 13−15 are formally spin-forbidden and therefore might also be expected to be better described by the use of eq 1 with $m = 1.5$:

$$Ni^+(^2D) + CS_2(^1\Sigma_g^+) \rightarrow NiS^+(^4\Sigma^-) + CS(^1\Sigma) \quad (13)$$

$$Cu^+(^1S) + COS(^1\Sigma) \rightarrow CuS^+(^3\Sigma^-) + CO(^1\Sigma) \quad (14)$$

$$Cu^+(^1S) + CS_2(^1\Sigma_g^+) \rightarrow CuS^+(^3\Sigma^-) + CS(^1\Sigma) \quad (15)$$

Table 3 includes such analyses of each of these reactions in comparison with analyses using $m = 1$. The results indicate that the choice of m does influence the optimized value of n, while the threshold energies remain relatively constant. This indicates that the flexibility of eq 1 and the parameter n can compensate for explicit changes in the parameter m. Therefore, the results of this and previous work[5,7] suggest that in most cases there is no significant difference between the thermochemistry obtained using $m = 1$ and 1.5. However, the reproduction of the data over extended energy regions is improved with $m = 1.5$ in some cases, especially for cross sections that rise rapidly.

The cross section for $[Ni,C,O]^+$ formation in reaction 16 begins near 1.5 eV and is much smaller than the dominant NiS^+ channel (Figure 8):

$$Ni^+ + COS \rightarrow [Ni,C,O]^+ + S \quad (16)$$

Using $D_0(Ni^+-CO) = 1.81 \pm 0.11$ eV,[34] the expected threshold for $NiCO^+$ formation according to reaction 16 is 1.33 ± 0.11 eV. Analysis of the present data yields an average threshold of 1.77 ± 0.16 eV, somewhat above the value based on the literature thermochemistry. This difference is likely a result of competition with the lower energy process, reaction 12. This cross section reaches a maximum close to the energy predicted for the onset of reaction 11.

Discussion

Thermochemistry of Metal Sulfide Cations. As described above, independent determinations of $D_0(Cu^+-S) = 1.81 \pm 0.09$ and 2.07 ± 0.15 eV are derived from the CuS^+ thresholds in the reactions with CS_2 and COS, respectively. The agreement between these values is disappointing; however, our determination of the CuS^+ threshold in the CS_2 reaction is probably less accurate than that obtained from the COS reaction. In the CS_2 system, this is because the early onset of the competitive $CuCS^+$ channel may shift the CuS^+ threshold to higher energies. Previous studies have demonstrated this effect for competing reaction pathways.[35] In the COS system, the analogous $CuCO^+$ product channel has a higher threshold than CuS^+ formation, such that no competition occurs. We therefore report a value of $D_0(Cu^+-S) = 2.07 \pm 0.15$ eV, which is derived exclusively from the COS reaction. This value differs from a previously reported value[3,36] that was obtained from a preliminary analysis of the CS_2 reaction system alone.

The NiS^+ thresholds from the CS_2 and COS reactions are similarly used to calculate values of $D_0(Ni^+-S) = 2.30 \pm 0.09$ and 2.46 ± 0.04 eV, respectively. Similar to the Cu^+/CS_2 system, the $NiCS^+$ product has a lower threshold (2.07 ± 0.09 eV) than the NiS^+ threshold (2.20 ± 0.08 eV) in the reaction of Ni^+ with CS_2. Competition in the Ni^+/CS_2 system may therefore shift the NiS^+ threshold to slightly higher energies, leading to a lower bond energy, as previously reported.[3,36] The case for rejecting the $D_0(Ni^+-S)$ value derived in the $Ni^+ + CS_2$ reaction is not as strong as in the analogous Cu^+ system. Figure 1 shows that the apparent thresholds are close in energy, whereas the $CuCS^+$ cross section in Figure 2 clearly rises before that of CuS^+. Additionally, the discrepancy of 0.16 ± 0.10 eV between the derived NiS^+ bond energies is smaller than that observed for the CuS^+ bond energies (0.26 ± 0.17 eV). Nevertheless, competition seems to affect the results, and therefore, we report the value of $D_0(Ni^+-S) = 2.46 \pm 0.04$ eV derived in the reaction with COS. This value is in excellent agreement with a recent value of 2.47 ± 0.04 eV derived from photodissociation spectra.[37]

The bond energies determined from the ZnS^+ thresholds in the reactions of Zn^+ with CS_2 and COS are 2.05 ± 0.14 and 2.05 ± 0.12 eV, respectively. These values are in excellent agreement, and we report a final value of $D_0(Zn^+-S) = 2.05 \pm 0.12$ eV. This good agreement is reasonable considering that competition with other channels should not affect the threshold for ZnS^+ formation in either system. This value is within experimental error of a previously reported value[3,36] that was derived exclusively from preliminary analysis of the CS_2 reaction system.

These values can be converted to 298 K values using frequency calculations performed at the B3LYP/6-311+G* level which find 374 cm^{-1} for NiS^+, 338 cm^{-1} for CuS^+, and 382 cm^{-1} for ZnS^+. In all cases, the correction from 0 to 298 K is approximately 0.04 eV giving 298 K bond energies of 2.50 ± 0.08, 2.11 ± 0.15, and 2.09 ± 0.12 eV, respectively. The former value is in good agreement with 2.60 ± 0.22 eV obtained from earlier photodissociation studies of NiS^+.[38] In addition, these authors determined that NiS^+ reacts with ethane to form Ni^+ and, presumably, ethanethiol. The energy needed to extract an S atom from C_2H_5SH is 2.48 ± 0.01 eV at 298 K, which is a lower limit to the NiS^+ bond energy, assuming that the NiS^+ reactant ion examined in that particular study had no excessive internal excitation. This limit is in good agreement with the value derived here.

The trends in these bond energies are comparable to those observed for the transition metal oxide cations: $D_0(Ni^+-O) = 2.74 \pm 0.05$,[39,40] $D_0(Cu^+-O) = 1.62 \pm 0.16$,[39] and $D_0(Zn^+-O) = 1.67 \pm 0.05$ eV.[39,41] Similar to other later 3d metals, Mn, Fe, and Co,[3,7-10] the nickel-oxide cation bond energy is stronger than that of the nickel−sulfide cation (with a difference of ~0.4 eV for all four metals). In contrast, the sulfide bond energies of copper and zinc cations exceed those of the oxides, and both the sulfide and oxide cation bonds of these metals are substantially weaker than those of nickel. These results can be rationalized if the CuX^+ and ZnX^+ bonds are largely electrostatic, as previously suggested for the oxides.[23] Accordingly, the interactions are no longer truly covalent, such that the bonds are weaker. For electrostatic interactions, the relative stabilities of the sulfides and oxides will be related to the polarizabilities of the sulfur and oxygen ligand, 2.90 and 0.802 $Å^3$, respectively,[42] consistent with stronger bonds to sulfur. Further, such electrostatic interactions can reasonably lead to very similar bond energies, as observed for copper and zinc.

Another approach to understanding the bonding in the MS^+ systems is to examine the valence molecular orbitals (MOs) that arise in these molecules using LCAO-MO theory (core orbitals are ignored in the numbering scheme used here so that the similarities in sulfur and oxygen can be emphasized). To a first approximation, the 3s orbital of sulfur (or 2s on oxygen) constitutes the 1σ orbital, the 4s and 3d orbitals on the metal combine with the 3p orbitals on sulfur (or 2p on oxygen) to form 2σ and 1π bonding orbitals, 1δ and 3σ nonbonding orbitals, and 2π and 4σ antibonding orbitals. The ground states of NiS^+ and NiO^+ are found to be high-spin $^4\Sigma^-$ states with a $1\sigma^2 2\sigma^2 1\pi^4 1\delta^4 3\sigma^1 2\pi^2$ valence electron configuration.[3,43,44] Because the 3σ and 2π orbitals are close in energy, the high-spin

configuration is preferred in order to maximize the electron exchange energy. In essence, this configuration is a covalent double bond (a σ bond, two π bonds, and two antibonding π electrons). The addition of another electron for Cu^+ results in $1\sigma^2 2\sigma^2 1\pi^4 1\delta^4 3\sigma^2 2\pi^2$ valence electron configurations for CuS^+ and CuO^+ with $^3\Sigma^-$ ground states.[36,44,45] However, the increased nuclear charge means that the 2σ, 1π, and 1δ orbitals are largely metal-based 3d core orbitals, meaning that there is only a single dative bond between $Cu^+(^1S)$ and $S(^3P)$ or $O(^3P)$. Moving to Zn^+ gives $1\sigma^2 2\sigma^2 1\pi^4 1\delta^3 3\sigma^2 2\pi^3$ valence electron configurations for ZnS^+ and ZnO^+ and $^2\Pi$ ground states,[44,45] where the 2σ, 1π, and 1δ orbitals are again mainly metal-based 3d orbitals, resulting in a single dative bond.

Thermochemistry of Metal Thio-Carbonyl Cations. The thresholds for forming the MCS^+ product in the reactions of Ni^+, Cu^+, and Zn^+ with CS_2 (Table 3) lead to $D_0(Ni^+-CS) = 2.43 \pm 0.10$, $D_0(Cu^+-CS) = 2.47 \pm 0.12$, and $D_0(Zn^+-CS) = 1.54 \pm 0.24$ eV, respectively. As mentioned above, the value of $D_0(Cu^+-CS) = 2.47 \pm 0.12$ eV derived from the CS_2 reaction is considerably larger than the value of $D_0(Cu^+-CO) = 1.57 \pm 0.32$ derived in the reaction with COS. Similarly, $D_0(Ni^+-CS) = 2.43 \pm 0.10$ derived in this work is larger than the previously reported value of $D_0(Ni^+-CO) = 1.81 \pm 0.11$ eV.[34,46] The M^+-CS interactions are enhanced relative to the M^+-CO interactions for several reasons. One explanation deals with the polarizability of the CS ligand, which is unknown but certainly exceeds that of CO (1.94 Å^3)[47] considering the polarizabilities of CS_2 (9.1 Å^3), COS (5.7 Å^3), and CO_2 (2.9 Å^3).[48] Additionally, an analysis of the molecular orbital schemes of CS and CO reveals that the σ-donor and π-acceptor orbitals of CS are lower in energy than those of CO.[3] Both factors enhance the metal-to-carbon interaction of the MCS^+ species over that of the MCO^+ species.

Interestingly, the derived value of $D_0(Zn^+-CS)$[49] is less than two-thirds of $D_0(Ni^+-CS)$ and $D_0(Cu^+-CS)$. This implies that the formal bond order of $ZnCS^+$ is less than that of $NiCS^+$ and $CuCS^+$, consistent with the bonding nature of CS to metals. The CS ligand forms a strong σ bond by donating the electron pair on the C atom into an empty σ-type orbital of the metal. Electron density from the metal is then back-donated into the π antibonding orbitals of CS. Because Zn^+ has a $3d^{10}4s^1$ electron configuration, there is no empty orbital to accept the electron pair of CS. The 4s electron must be promoted to an antibonding orbital, causing a weaker M^+-CS interaction. By contrast, both Ni^+ and Cu^+ have $3d^n$ configurations with empty 4s orbitals into which the electron pair of CS can be donated. This line of reasoning explains the observed order $D_0(Ni^+-CS) \sim D_0(Cu^+-CS) > D_0(Zn^+-CS)$. Note that analogous considerations should hold for the metal carbonyl cations, such that the Zn^+-CO bond energy should be particularly weak, thereby explaining the failure to observe this product in the reaction of Zn^+ with COS.

Reaction Mechanism. The overall behavior of the M^+/CS_2 and M^+/COS systems suggests that M^+ ions activate CXS by inserting into the C−S bond to form the corresponding $S-M^+-CX$ intermediates. Results of the analogous reactions of CS_2 with V^+, Cr^+, Mn^+, Fe^+, and Co^+ are consistent with the formation of an $S-M^+-CS$ intermediate,[5,7,10] as are ab initio calculations of the V^+/CS_2 potential-energy surface.[5] All of the observed products can be formed by cleavage of specific bonds of this key intermediate. Thus, cleavage of the SM^+-CS and $S-MCS^+$ bonds provide low-energy routes to formation of MS^+ and MCS^+ according to reactions 2 and 3, respectively. Cleavage of the SMC^+-S bond leads to the inserted $S-M^+-C$ species, which can further decompose to yield MS^+. Likewise, involvement of $S-M^+-CO$ can account for the experimental observations in the COS systems. Here, insertion into the C−S bond is more facile than in CS_2 because the bond is weaker. There is a substantially reduced probability of inserting into the C−O bond to form the $O-M^+-CS$ intermediate, because of the large difference in the C−O and C−S bond energies (6.88 vs 3.14 eV).[5,7] Thus, MS^+ and MCO^+ species dominate as products, whereas the alternative product ions, MO^+ and MCS^+, are not formed in sufficient abundances to be observed for M = Ni, Cu, and Zn.

Summary

The reactions of Ni^+, Cu^+, and Zn^+ with CS_2 and COS are studied using guided ion beam mass spectrometry. The results indicate that a dc discharge produces measurable quantities of the $Ni^+(^4P)$ third excited state and the $Cu^+(^3D)$ first excited state. Whereas these states are resistant to collisional quenching by helium and argon in the flow tube, they can be largely eliminated from the M^+ ion beam by addition of adequate cooling gases (O_2 for Ni^+ and NO for Cu^+). In contrast, no evidence for excited-state Zn^+ was found, presumably because the excited states of Zn^+ are extremely high in energy (>6.08 eV, Table 2) and radiate rapidly.

The cross sections for MS^+ and MCX^+ formations in the M^+/CXS systems are consistent with initial activation of the neutral reactants by insertion of the metal ion into a CS bond to form $S-M^+-CX$ (X = S, O) intermediates from which all subsequent products evolve. High-energy endothermic features in the $[Zn,C,S]^+$ and $[Cu,C,O]^+$ cross sections of these systems suggest the possible formation of metal-inserted, $S-Zn^+-C$ and $O-Cu^+-C$, or cyclic isomers, but excited electronic states of the more conventional $Zn^+(CS)$ and $Cu^+(CO)$ complexes seem more likely for these metals.

The cross section for NiS^+ formation in the reaction with COS exhibits an unusual decline, which is attributed to the energy dependence of the surface crossing probability in this spin-forbidden process. The modeling results for the spin-forbidden formations of NiS^+ and CuS^+ in the reactions with CS_2 and COS indicate that $m = 1.0$ and 1.5 yield nearly identical thresholds for these systems. However, the reproduction of the data over a wide energy range is superior using $m = 1.5$ in cases where the cross sections of formally spin-forbidden reactions rise rapidly from threshold.

Finally, the threshold values of the various product cross sections are used to determine $D_0(Ni^+-S) = 2.46 \pm 0.04$, $D_0(Ni^+-CS) = 2.43 \pm 0.10$, $D_0(Cu^+-S) = 2.07 \pm 0.15$, $D_0(Cu^+-CS) = 2.47 \pm 0.12$, $D_0(Zn^+-S) = 2.05 \pm 0.12$, and $D_0(Zn^+-CS) = 1.54 \pm 0.24$ eV. Careful evaluation of the data shows that competition between product channels can raise the measured threshold of the higher-energy processes in some systems, leading to bond energies that are potentially too low. Thus, the bond energies, $D_0(Ni^+-S)$ and $D_0(Cu^+-S)$, are derived exclusively from the Ni^+/COS and Cu^+/COS systems, in which MS^+ formation is not affected by a competitive product channel. This finding highlights the need for an appropriate description of competing processes when accurate gas-phase thermochemistry is to be derived from guided ion beam experiments. In a more general sense, we note that similar considerations concerning competitive dissociations almost certainly apply for the various kinds of thermokinetic approaches[50] that are frequently used in gas-phase ion chemistry.

Acknowledgment. This work is supported by the National Science Foundation, Grant No. CHE-9877162 and CHE-

0135517. The Berlin group acknowledges support by the Deutsche Forschungsgemeinschaft, the Volkswagen-Stiftung, and the Fonds der Chemischen Industrie.

References and Notes

(1) Stiefel, E. I. In *Transition Metal Sulfur Chemistry*; Stiefel, E. I., Matsumoto, K., Eds.; ACS Symposium Series 653; American Chemical Society: Washington, DC, 1996; pp 2−38, and references therein.

(2) (a) Takakuwa, S. In *Organic Sulfur Chemistry, Biochemical Aspects*; Oae, S., Okyama, T., Eds.; CRC Press: Boca Raton, FL, 1992. (b) Lippard, S. J.; Berg, J. M. *Principles of Bioinorganic Chemistry*; University Science Books: Mill Valley, CO, 1994. (c) Rehder, D. *Angew. Chem., Int. Ed.* **1991**, *30*, 148. (d) Butler, A.; Carrano, C. J. *Coord. Chem. Rev.* **1991**, *109*, 61. (e) Solomon, E. I.; Chen, P.; Metz, M.; Lee, S. K.; Palmer, A. E. *Angew. Chem.* **2001**, *113*, 4702; *Angew. Chem., Int. Ed.* **2001**, *40*, 4570.

(3) For a general discussion of the periodic trends of first and second-row transition-metal sulfides, see: Kretzschmar, I. Ph.D. Thesis, Technische Universität Berlin D83, 1999. Published as *Energetics and Reactivity of the Binary Transition-Metal Sulfides of the 3rd and 4th Row*; Shaker Verlag: Aachen, 1999.

(4) Kretzschmar, I.; Schröder, D.; Schwarz, H.; Rue, C.; Armentrout, P. B. *J. Phys. Chem. A* **2000**, *104*, 5046.

(5) Rue, C.; Armentrout, P. B.; Kretzschmar, I.; Schröder, D.; Harvey, J. N.; Schwarz, H. *J. Chem. Phys.* **1999**, *110*, 7858.

(6) Kretzschmar, I.; Schröder, D.; Schwarz, H.; Rue, C.; Armentrout, P. B. *J. Phys. Chem.* **1998**, *102*, 10060.

(7) Rue, C.; Armentrout, P. B.; Schröder, D.; Kretzschmar, I.; Schwarz, H. *Int. J. Mass Spectrom.* **2001**, *210/211*, 283.

(8) Harvey, J. N.; Heinemann, C.; Fiedler, A.; Schröder, D.; Schwarz, H. *Chem. Eur. J.* **1996**, *2*, 1230.

(9) Schröder, D.; Kretzschmar, I.; Schwarz, H.; Rue, C.; Armentrout, P. B. *Inorg. Chem.* **1999**, *38*, 3474.

(10) Rue, C.; Armentrout, P. B.; Schröder, D.; Kretzschmar, I.; Schwarz, H. *J. Phys. Chem. A* **2001**, *105*, 8456.

(11) Ervin, K. M.; Armentrout, P. B. *J. Chem. Phys.* **1985**, *83*, 166.

(12) Schultz, R. H.; Armentrout, P. B. *Int. J. Mass Spectrom. Ion Processes* **1991**, *107*, 29.

(13) Armentrout, P. B. In *Advances in Gas-Phase Ion Chemistry*; Adams, N. G., Babcock, L. M., Eds.; JAI: Greenwich, 1992; pp 83−119, Vol. 1.

(14) Kickel, B. L.; Armentrout, P. B. *J. Phys. Chem.* **1995**, *99*, 2024.

(15) (a) Khan, F. A.; Steele, D. L.; Armentrout, P. B. *J. Phys. Chem.* **1995**, *99*, 7819. (b) Chen, Y.-M.; Armentrout, P. B. *J. Chem. Phys.* **1995**, *103*, 618. (c) Haynes, C. L.; Armentrout, P. B. *Organometallics* **1994**, *13*, 3480. (d) Fisher, E. R.; Kickel, B. L.; Armentrout, P. B. *J. Chem. Phys.* **1992**, *97*, 4859. (e) Kemper, P. R.; Bowers, M. T. *J. Phys. Chem.* **1991**, *95*, 5134.

(16) Kickel, B. L.; Armentrout, P. B. *J. Am. Chem. Soc.* **1995**, *117*, 764.

(17) Rodgers, M. T.; Walker, B.; Armentrout, P. B. *Int. J. Mass Spectrom. Ion Processes* **1999**, *182/183*, 99.

(18) Sunderlin, L. S.; Armentrout, P. B. *J. Phys. Chem.* **1988**, *92*, 1209.

(19) (a) Garstang, R. H. *Mon. Not. R. Astron. Soc.* **1962**, *124*, 321. (b) Russel, D. H.; Oriedo, J. V. B.; Solouki, T. In *Organometallic Ion Chemistry*; Freiser, B. S., Ed.; Kluwer Academic: Dordrecht, The Netherlands, 1996; p 197−228, and references therein.

(20) Werner, H. *Angew. Chem.* **1990**, *102*, 1109; *Angew. Chem., Int. Ed. Engl.* **1990**, *29*, 1077.

(21) Lias, S. G. Ionization Energy Data. In *NIST Chemistry WebBook, NIST Standard Reference Database Number 69*; Linstrom, P. J., Mallard, W. G., Eds.; National Institute of Standards and Technology: Gaithersburg, MD, 2001 (http://webbook.nist.gov).

(22) Elkind, J. L.; Armentrout, P. B. *J. Chem. Phys.* **1986**, *84*, 4862.

(23) Fisher, E. R.; Elkind, J. L.; Clemmer, D. E.; Georgiadis, R.; Loh, S. K.; Aristov, N.; Sunderlin, L. S.; Armentrout, P. B. *J. Chem. Phys.* **1990**, *93*, 2676.

(24) http://physics.nist.gov/cgi-bin/AtData/main_asd.

(25) Herzberg, G. *Molecular Spectra and Molecular Structure*, 2nd ed.; Van Nostrand: New York, 1950; Vol. 1.

(26) Gioumousis, G.; Stevenson, D. P. *J. Chem. Phys.* **1958**, *29*, 294.

(27) Sugar, J.; Corliss, C. *J. Phys. Chem. Ref. Data* **1985**, *14*, Suppl. 2.

(28) Weber, M. E.; Elkind, J. L.; Armentrout, P. B. *J. Chem. Phys.* **1986**, *84*, 1521.

(29) Meyer, F.; Chen, Y.-M.; Armentrout, P. B. *J. Am. Chem. Soc.* **1995**, *117*, 4071.

(30) (a) Barnes, L. A.; Rosi, M.; Bauschlicher, C. W. *J. Chem. Phys.* **1990**, *93*, 609. (b) See also: Lupinetti, A. J.; Fau, S.; Frenking, G.; Strauss, S. H. *J. Phys. Chem. A* **1997**, *101*, 9551.

(31) Stowe, G. F.; Schultz, R. H.; Wight, C. A.; Armentrout, P. B. *Int. J. Mass Spectrom. Ion Processes* **1990**, *100*, 177.

(32) Heller, E. J.; Brown, R. C. *J. Chem. Phys.* **1983**, *79*, 3336.

(33) Lorquet, J. C.; Leyh-Nihant, B. *J. Phys. Chem.* **1988**, *92*, 4778.

(34) (a) Armentrout, P. B.; Kickel, B. L. In *Organometallic Ion Chemistry*; Freiser, B. S., Ed.; Kluwer Academic: Dordrecht, The Netherlands, 1996; p 28. (b) Khan, F. A.; Steele, D. A.; Armentrout, P. B. *J. Phys. Chem.* **1995**, *99*, 7819.

(35) Rodgers, M. T.; Armentrout, P. B. *J. Chem. Phys.* **1998**, *105*, 1787.

(36) Kretzschmar, I.; Schröder, D.; Schwarz, H.; Armentrout, P. B. In *Advances in Metal and Semiconductor Clusters*; Duncan, M. A., Ed.; Elsevier Science B.V.: New York, 2001; Vol. 5, pp 347−395.

(37) Husband, J.; Aguirre, F.; Thompson, C. J.; Metz, R. B. *Chem. Phys. Lett.* **2001**, *342*, 75.

(38) Jackson, T. C.; Carlin, T. J.; Freiser, B. S. *Int. J. Mass Spectrom. Ion Processes* **1986**, *72*, 169.

(39) Fisher, E. R.; Elkind, J. L.; Clemmer, D. E.; Georgiadis, R.; Loh, S. K.; Aristov, N.; Sunderlin, L. S.; Armentrout, P. B. *J. Chem. Phys.* **1990**, *93*, 2676.

(40) Fisher, E. R.; Armentrout, P. B. *J. Phys. Chem.* **1990**, *94*, 1674.

(41) Clemmer, D. E.; Dalleska, N. F.; Armentrout, P. B. *J. Chem. Phys.* **1991**, *95*, 7263.

(42) Miller, T. M.; Bederson, B. *Adv. At. Mol. Phys.* **1977**, *13*, 1.

(43) Fiedler, A.; Hrušák, J.; Koch, W.; Schwarz, H. *Chem. Phys. Lett.* **1993**, *211*, 242.

(44) Fiedler, A.; Schröder, D.; Shaik, S.; Schwarz, H. *J. Am. Chem. Soc.* **1994**, *116*, 10734.

(45) Schröder, D.; Schwarz, H.; Shaik, S. *Structure and Bonding*; Springer-Verlag: Heidelberg, Germany, 2000; Vol. 97, p 91.

(46) Khan, F. A.; Steele, D. A.; Armentrout, P. B. *J. Phys. Chem.* **1995**, *99*, 7819.

(47) Rothe, E. W.; Bernstein, R. B. *J. Chem. Phys.* **1959**, *31*, 1619.

(48) Spackman, M. A. *J. Phys. Chem.* **1989**, *93*, 7594, and references therein.

(49) The value of $D_0(Zn^+-CS)$ reported here is potentially subject to a threshold measurement error because of the competitive effect of the ZnS^+ cross section. If $ZnCS^+$ formation is suppressed by the competitive formation of ZnS^+, the true threshold for $ZnCS^+$ formation will be lower than the reported value, and the true bond energy will be correspondingly higher. In the Ni^+/CS_2 and Cu^+/CS_2 systems, the threshold for MCS^+ formation is lower in energy than that of MS^+ formation, so the derived thermochemistry is expected to be accurate.

(50) (a) Cooks, R. G.; Wong, P. S. H. *Acc. Chem. Res.* **1998**, *31*, 379. (b) Bouchoux, G.; Leblanc, D.; Sablier, M. *Int. J. Mass Spectrom.* **2001**, *210/211*, 189 and references therein.